Body map proto-organization in newborn macaques

Michael J. Arcaro[a,b,1], Peter F. Schade[b], and Margaret S. Livingstone[b]

[a]Department of Psychology, University of Pennsylvania, Philadelphia, PA 19104; and [b]Department of Neurobiology, Harvard Medical School, Boston, MA 02115

Topographic sensory maps are a prominent feature of the adult primate brain. Here, we asked whether topographic representations of the body are present at birth. Using functional MRI (fMRI), we find that the newborn somatomotor system, spanning fronto-parietal cortex and subcortex, comprises multiple topographic representations of the body. The organization of these large-scale body maps was indistinguishable from those in older monkeys. Finer-scale differentiation of individual fingers increased over the first 2 y, suggesting that topographic representations are refined during early development. Last, we found that somatomotor representations were unchanged in 2 visually impaired monkeys who relied on touch for interacting with their environment, demonstrating that massive shifts in early sensory experience in an otherwise anatomically intact brain are insufficient for driving cross-modal plasticity. We propose that a topographic scaffolding is present at birth that both directs and constrains experience-driven modifications throughout somatosensory and motor systems.

somatosensory | motor | macaque | development | proto-organization

Smooth and continuous representations of the sensory periphery, i.e., topographic maps, are a fundamental feature of information processing in the adult primate brain (1). Topographic maps cover most of the adult cortical surface. The adult primate somatosensory and motor systems comprise several areas spanning parietal and frontal cortices, as well as subcortex. Each area contains some combination of mechanosensory, proprioceptive, and muscle representations of the body that, at a large scale, are topographically organized into multiple maps of the body (2–6). This large-scale organization, as well as the anatomical and functional properties of individual areas, are similar across individuals, suggesting a common program for their development. However, the mechanisms guiding such organization remain unresolved. Prior microelectrode recordings in newborn macaques found neurons in primary somatosensory cortex (3a/b) to be unresponsive to tactile stimulation and immature in infant marmosets (7). Furthermore, area 1, which processes information from area 3b (8), was less responsive in newborns than in older monkeys, all of which suggests that the primate somatomotor system is functionally immature at birth. Beyond these early somatosensory areas, the functional organization of the somatomotor hierarchy at birth has yet to be explored. Here, we ask whether representations of the body are present in neonates, and to what extent does the organization of the infant somatomotor system resemble that found in older monkeys.

Results

Cortical Responses to Tactile Stimulation in Newborns and Juveniles. We performed somatotopic (tactile body) mapping using contrast-based (monocrystalline iron oxide nanoparticle [MION]) functional MRI (fMRI) in 9 monkeys ranging in age from 11 to 981 d. During scanning, the monkeys were fully alert. Each monkey was scanned once. Comparisons were made across individuals as well as between newborn (<18-d) and juvenile (>1-y-old) age groups (Table 1). The face (cheek), (glabrous) hands, and (glabrous) feet were stimulated unilaterally in a blocked design (*Materials and Methods*, *Tactile Stimulation*). Each monkey exhibited robust cortical activity during tactile stimulation of the contralateral face,

hand, and foot (P < 0.0001, uncorrected; *SI Appendix*, Fig. S1). Activity was observed on both the posterior (primary somatosensory) and anterior (primary motor) banks of the central sulcus and varied systematically along the dorsal/ventral axis, with face responses localized to focal spots ventrally, foot responses covering the dorsal-most regions, and hand responses falling in between. These activity patterns from contralateral stimulation were consistent across monkeys (Fig. 1, middle row; *SI Appendix*, Fig. S1, bottom row). For a subset of monkeys, the lower back was also stimulated (*SI Appendix*, Fig. S1). Evoked activity from lower back stimulation partially overlapped activity from stimulation of the foot but was also found further ventral within the central sulcus, above the hand representation. The relative locations of face, hand, back, and foot responses are consistent with prior electrophysiology, fMRI, and stimulation studies in macaques demonstrating spatially distinct representations of the face, hand, and foot within primary somatosensory (9–14) and motor cortex (4, 15, 16). Even in the youngest monkey tested (M1, 11 d), this evoked activity was found within the central sulcus (*SI Appendix*, Fig. S1), demonstrating that neonatal primary somatomotor cortex already exhibits spatially specific representations of the body.

Although each monkey was head restrained, their bodies could move freely within the primate chair. Head motion during scans was minimal and control analyses suggest that any distortions from brief, large movements were unlikely to produce condition-related biases (*SI Appendix, Assessing head motion*). Body movements, however, likely yielded significant motor-related activity (*SI Appendix, Motor-cortex activation during stimulation*). Importantly, the evoked activity within primary somatosensory and motor areas were localized to similar locations along the dorsal-ventral axis,

Significance

This study reports the discovery that large-scale topographic maps of the body exist throughout the entire primate somatosensory and motor systems at birth. Our results suggest that this proto-organization is established prenatally, even in areas that are crucial for coordinating and executing complex, ethologically relevant actions in adults. Given the behavioral immaturity of neonates, this suggests that large-scale body maps precede these action domains. Furthermore, our data can explain how these domains arise in stereotypical locations without the need for prespecification of function. This study demonstrates that topographic representations are a fundamental and pervasive principle of early development, providing the protoarchitecture of the entire brain on which experience-dependent specializations are elaborated postnatally.

NEUROSCIENCE

Table 1. Individual monkey scanning information for face, hand, and foot stimulation

Monkey	Age, d	Stimulation paradigm	Body side stimulated	Hemisphere examined
M1	11	Air puff to face, manual stroke to hands and feet	Right side only	Both (unilateral GLM analysis)
M2	17	Air puff to face, manual stroke to hands and feet	Right side only	Both (unilateral GLM analysis)
M3	39	Air puff to face, manual stroke to hands, feet and lower back	Both	Both
M4	146	Air puff to face, manual stroke to hands, feet and lower back	Both	Both
M5	426	Air puff to face, manual stroke to hands, feet and lower back	Both	Both
M6	438	Air puff to face, manual stroke to hands, feet and lower back	Both	Both
M7	586	Air puff to face, manual stroke to hands, feet and lower back	Both	Both
M8	669	Air puff to face, manual stroke to hands, feet and lower back	Both	Both
M9	981	Air puff to face, hands, and feet	Both	Both

reflecting the general alignment of somatosensory and motor maps, and indicating that tactile- and motor-related stimulation drove activity in cortical regions representing the same part of the body.

Because the alert monkeys could move their bodies freely in the chair, there was doubtless both motor and somatosensory stimulation that would not be captured in our regression analysis. To better detect brain areas that reflect all activity related to each body part, we conducted an independent component analysis (ICA) on the data (*Materials and Methods, ICA*). This data-driven approach can identify significant structure in the data not restricted to the condition blocks. Spatial activity maps were then reconstructed from each independent component to visualize the regions of the brain whose signals most contributed to each component. Components corresponding to the foot, hand, and face regions within the central sulcus were identified in each

monkey (Fig. 1, bottom row, and *SI Appendix*, Fig. S2) by correspondence with the group average activation (beta) maps and in reference to prior studies in adults (3, 17). For each monkey, there was a strong correlation between the group average activity (beta) map from the regression analysis and the independent component (IC) map for both hands (mean spatial correlation within the central sulcus across monkeys; mean $r = 0.91 \pm 0.02$) and feet (mean $r = 0.83 \pm 0.03$). The group average face activity map was also correlated with the face IC map for each monkey (mean $r = 0.52, \pm 0.03$); however, each face IC covered a larger extent of the cortical surface. In each monkey, the face IC map included the focal ventral region of activity in the group average face beta maps, but was more extensive, encompassing approximately the entire ventral third of the central sulcus. We attribute this difference to the fact that the monkey's head and face were continuously stimulated throughout each scan, including baseline
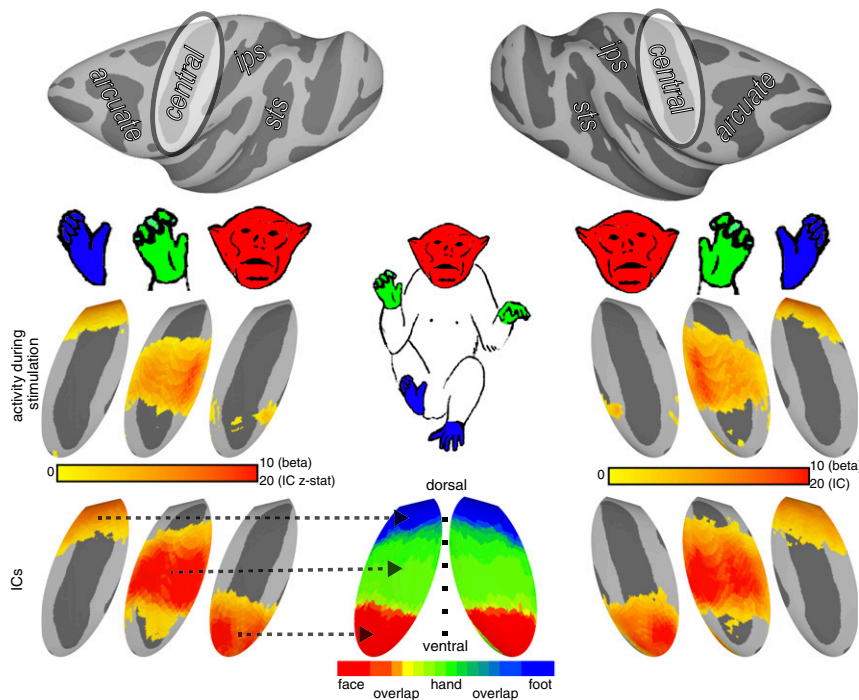

Fig. 1. Topographic organization of primate central sulcus in young monkeys. Spatially specific activity within the central sulcus were observed during stimulation of the contralateral foot, hand, and face from both (middle row) GLM (beta values) and (bottom row) independent component (IC) analyses. Group average ($n = 9$ in right hemisphere and $n = 7$ in the left hemisphere) data show vertices that were significantly active in the beta ($P < 0.0001$, uncorrected) and IC (z stat > 4.0) maps in at least 4 subjects from a conjunction analysis (*SI Appendix*, Fig. S1). (Bottom row, *Middle*) Combined, these activity maps formed an inverted topographic gradient of body representations symmetric between the hemispheres with the face (red) represented ventrally, feet (blue) represented dorsally, and a large hand representation (green) in between. Overlap between face and hand IC maps were represented as a gradient between red and green in RGB color space. Overlap between hand and foot IC maps were represented as a gradient between green and blue in RGB color space. The arrows indicate the correspondence between each body IC map to the topographic map. Monkey illustrations adapted from ref. 59, with permission from Elsevier.

periods, from the helmet restraint and receipt of periodic juice reward. This was confirmed in a control experiment in which the mouth, tongue, and teeth were stimulated via juice delivery in a blocked design. Juice-related activity was observed throughout the ventralmost portion of the central sulcus and covered most of the face IC map (*SI Appendix*, Fig. S3). Indeed, this additional ventral part of the central sulcus is known to represent the mouth, teeth, and tongue in adults (18). In contrast to the lateralized hand and foot IC maps, face IC maps were bilateral and symmetric in every monkey. This may reflect the denser callosal interconnectivity between mouth, teeth, and tongue representations (vs. foot and hand) in primary somatosensory cortex (19) or bilateral representations of the teeth and other intraoral structures (18, 20), but also may reflect costimulation of both sides of the face from rubbing against the helmet and receiving juice rewards. While the group average beta and IC maps were similar for each body part, the IC maps were more anatomically consistent across individuals (the variance across subjects in the spatial similarity of IC maps was less than one-half the variance for the beta maps).

Topographic Organization of Primary Somatomotor Cortex in Newborns. A topographic map of the body was identified in newborn monkeys as early as 11 d of age (Fig. 2). To identify topographic body maps, the weights of face, hand, and foot ICs were used to derive the region of the body each voxel most strongly represented (*Materials and Methods, Body Map Analysis*). Consistent with the activity maps for individual body parts, a large-scale topographic gradient of body part representations was identified within the central sulcus spanning both anterior and posterior banks (Figs. 1, bottom row, and 2 and *SI Appendix*, Fig. S2). A large representation of the face (red) was identified in the ventral third of the central sulcus from the body map analysis. This face representation progressed to a hand representation (green) in the middle of the central sulcus and then to a representation of the foot dorsally (blue). There was minimal overlap between body representations (*SI Appendix, Overlap of body representations*). The anatomical locations of these face, hand, and foot representations within the central sulcus were consistent across all ages (Fig. 2 and *SI Appendix*, Fig. S2) and correspond to the established large-scale organization in adult monkeys from microelectrode recordings (*SI Appendix*, Fig. S4A). Notably, the face beta maps fall within a cortical region known to represent the specific area of the face stimulated during tactile mapping (on the cheek between the upper lip and nose), whereas the face IC (and face representation in the gradient map) encompass face, mouth, and tongue representations in adults (3). This is consistent with our interpretation

that, in addition to the air puffs, the ICA captured evoked activity from the helmet and juice reward. Together, these data demonstrate the presence of a large-scale topographic map of the body within primary somatosensory and motor cortex of newborn monkeys.

Topographic Organization of Higher-Order Somatomotor Cortex in Newborns. Beyond the central sulcus, cortical responses to stimulation of the face, hand, and foot were observed throughout motor, premotor, somatosensory, parietal, and insular cortex (*SI Appendix*, Fig. S5). Several whole-body topographic maps were identified in neonatal monkeys as early as 11 d of age (Fig. 3 and *SI Appendix*, Fig. S6). Surrounding the central sulcus representation (Fig. 3A, #1), additional topographic representations of the body were identified in both newborns (<18 d) and juveniles older than 1 y. A second gradient of body representations was identified within the upper bank of the lateral sulcus (Fig. 3A, #2), consistent with the known large-scale organization in adults (*SI Appendix*, Fig. S4B, and ref. 17). Starting from the face representation ventral to the central sulcus, representations of the hand and foot were identified posterior and ventrally in a smooth gradient that extended to the intersection of the upper and lower insula. Ventral and anterior to this gradient, a third body gradient was identified within the insula (Fig. 3A, #3), consistent with the known large-scale organization in adults (13). Starting from the face representation within the anterior insula, hand and foot representations were identified posteriorly and abutted the gradient in the lateral sulcus ventrally. Several additional partial body maps were identified. Anterior to the face representation within the central sulcus, a representation of the hand was identified within ventral portions of the arcuate sulcus (Fig. 3A, #4). Regions activated by stimulation of the feet more than hands and the face were not identified in most monkeys within the arcuate. Several representations of the hand and foot were identified adjacent to each other within medial parts of frontoparietal cortex (Fig. 3A, #5). The organization of these medial cortical body representations was complex, but similar across individuals. In most monkeys, regions activated by stimulation of the face more than hands and feet were not identified in midline regions of cortex. The critical result of these data is that the extent of these body representations was similar between newborns and juveniles, demonstrating that large-scale, topographic representations of the body across higher-order somatomotor cortex are already established in week-old monkeys and remain relatively unchanged compared to older monkeys.

NEUROSCIENCE
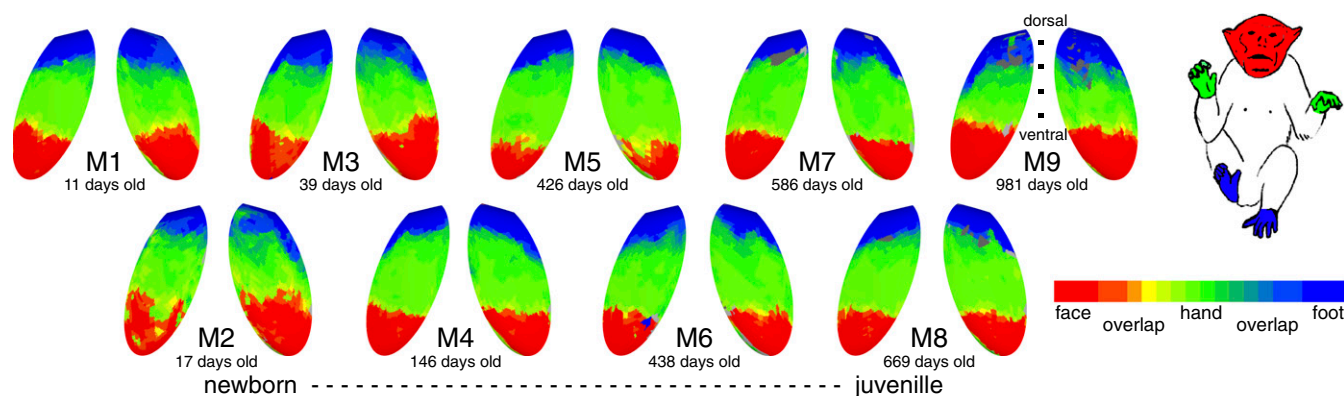
Fig. 2. A large-scale topographic gradient of body representations spanning primary somatosensory and motor cortex was present in every monkey. A large-scale topographic gradient of body representations spanning primary somatosensory and motor cortex was present in every monkey. Maps are shown for each monkey arranged by age from (left) M1 at 11 d old to (right) M9 at 981 d old. See Fig. 1 for additional conventions.

Arcaro et al.
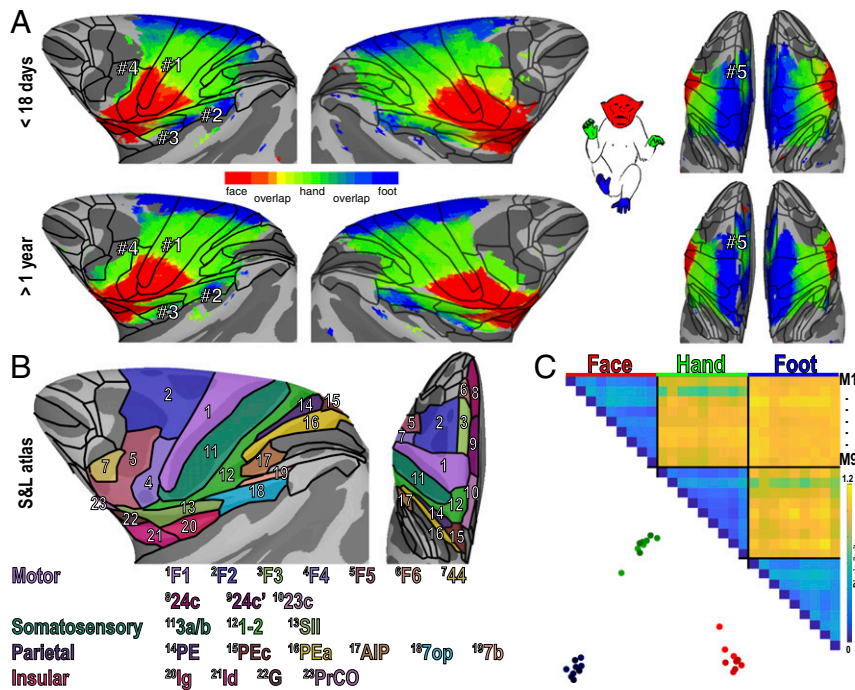
Fig. 3. Multiple body maps in newborns and juveniles. (*A*) Group average body maps of newborn (M1 and M2) and juvenile (M7 and M8) monkeys. Contralateral representations of the face, hand, and foot were found throughout frontal, anterior parietal, and insular cortex in monkeys younger than 18 d (M1 and M2) and in juveniles older than 1 y (M7 and M8). Several topographic gradients of body representations were observed in all monkeys. Data threshold at a group average z statistic > 4 for the strongest IC in each vertex. (*B*) Body representations overlapped with 23 areas of the Saleem and Logothetis atlas spanning motor, somatosensory, parietal, and insular cortex. (*C*) The spatial pattern of face, hand, and foot representations was consistent across all 9 monkeys tested. The dissimilarity matrix (1-corr) and MDS demonstrated that the spatial maps clustered based on body part stimulation, and there was no clear effect of age. For MDS, monkeys were luminance-coded by age from youngest (light) to oldest (dark). Face, hand, and foot representations were color coded red, green, and blue. See Fig. 1 for additional conventions.

Relation of Topographic Organization to Individual Cortical Areas.
Topographic gradients of body representations encompassed several motor, somatosensory, parietal, and insular cortical areas, based on an anatomical atlas (Fig. 3 *A* and *B*). Analogous to the multiple visual field maps that share a single eccentricity gradient, some of these large-scale topographic gradients may correspond to multiple, distinct body maps that run in parallel across the cortical surface with respect to face, hand, and foot representations. For example, the topographic gradient within the central sulcus (Fig. 3*A*, #1) spanned both primary motor cortex (F1/M1) and primary somatosensory cortex (3a/b and 1/2), which contain distinct maps of the body (4, 10). This topographic gradient also extended into neighboring areas in frontal cortex (F2) and anterior parietal cortex (PE, PEa, Pec, and AIP), which are also known to contain body representations (2, 3, 21–23). Other topographic gradients spanned several architectonic regions. The body representations within and around ventral portions of the arcuate (Fig. 3*A*, #4) spanned areas F4, F5, and 44, and the topographic gradient in the lateral sulcus (Fig. 3*A*, #2) spanned SII and 7op, consistent with prior electrophysiology studies in monkeys (17, 24–26). At least 2 body maps (SII and PV) can be differentiated within this region from fine-scale body mapping, although at the level of face, hand, and feet representations, run parallel and are difficult to differentiate (*SI Appendix*, Fig. S4*B* and ref. 3). It is also possible that some of these diverging body gradients correspond to a single, disjointed map as has been previously proposed for ventral and dorsal portions of premotor cortex (27). Higher imaging resolutions and finer body part mapping will be needed to differentiate the organization of individual maps within these gradients, including areas with fractured topography of repeating body parts such as F1/M1 (28, 29). Together, our data suggest a correspondence between the large-scale somatomotor functional gradients beyond primary cortex and anatomy that does not strictly adhere to architectonic borders.

Similarity of Topographic Organization across Ages.
The distribution of body part representations across cortex was consistent across individuals and ages (Fig. 3 and *SI Appendix*, Fig. S6). As shown in the similarity matrix (Fig. 3*C*), the spatial pattern of ICA maps computed across all voxels within the brain was more similar across individuals for matched (e.g., face IC of monkey M1 and face IC of monkey M6) than for nonmatched body parts (e.g., face IC of monkey M1 and hand IC of monkey M6). As shown in the multidimensional scaling (MDS) graph, data from individual monkeys clustered based on body part representation (Fig. 3*C*). There were no clear effects of age on the similarity of body part representations. The average spatial similarity between each monkey's IC map and all other monkeys was not significantly correlated with age of the monkey for hands and feet (r values < 0.08, P > 0.85). There was a moderate, but nonsignificant, correlation between the mean face IC similarity and age ($r = 0.51$, P > 0.16). The distribution of face, hand, and foot representations within architectonic regions was similar between newborn and juvenile monkeys for somatosensory, motor, parietal, and insular cortices (Fig. 4). These data confirm that stereotypical features of the adult body map organization are already present in newborns, including overrepresentations of the hand and face in primary somatosensory cortex: A larger portion of cortical real estate in newborns represents the hand and face compared to the feet (50% and 34% vs. 14%, respectively).

Topographic Organization of Subcortex in Newborns.
Body part gradient maps were also found throughout subcortex of newborns within the basal ganglia (putamen and globus pallidus) and

Arcaro et al.
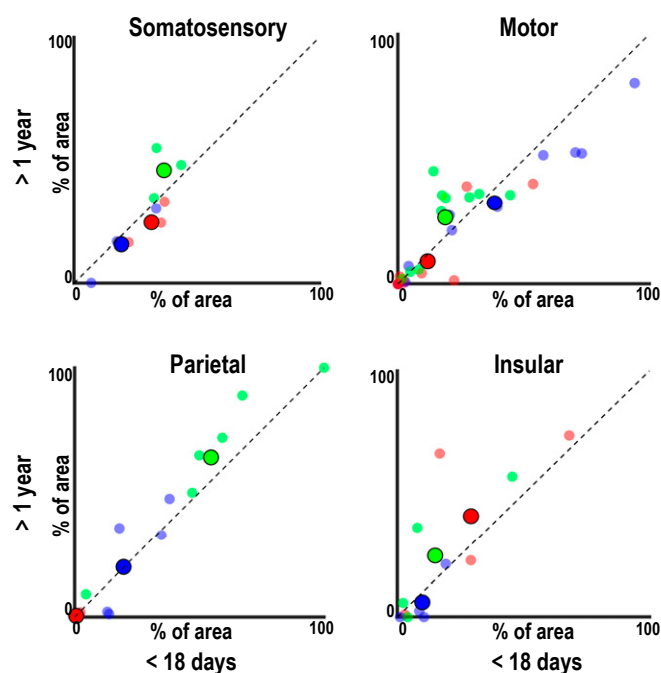
Fig. 4. Distribution of body representations across cortex in newborns (M1 and M2) and juveniles (M7 and M8). The cortical area comprising (red) face, (green) hand, and (blue) foot representations was comparable between newborns and juveniles for 23 cortical areas identified from the Saleem and Logothetis atlas (79) shown in Fig. 3 *A* and *B*. Large, black-outlined circles denote average body part representations (percentage of area) based on the grouping of the 23 cortical areas overlapping our somatomotor maps into broader somatosensory, motor, parietal, and insular cortical regions as shown in Fig. 3. Smaller circles denote average age group body part representations (percentage of area) within individual cortical areas.

posterior thalamus (Fig. 5). Similar to primary somatomotor cortex, each subcortical area contained an inverted topographic representation of the body with the face represented ventrally, hands represented in mid sections and feet dorsally. For posterior thalamic area VP, body representations varied also along the medial–lateral axis with face representations located in ventromedial-most portions and foot representations located in dorsolateral-most portions. Body representations extended dorsal and posterior of area VP, possibly corresponding to the anterior pulvinar nucleus or the "shell" region of VP (ventroposterior superior nucleus; refs. 30 and 31), although higher-resolution anatomical images would be required to differentiate these regions. All body representations in the thalamus were situated anterior to and were discrete from retinotopic maps within the ventral pulvinar (32). The distribution of face, hand, and foot representations within each region was similar between newborn and older juvenile monkeys, and was consistent with prior electrophysiological recordings and tracer studies in adult monkeys (6, 30, 33–38). Together, these data demonstrate the presence of large-scale topographic body maps in subcortical nuclei of newborn monkeys.

Postnatal Digit Maps. While the large-scale organization of the body is present at birth, the extent of the body represented by each neuron may be refined over the course of early development and therefore would be most apparent at a scale finer than face vs. hand vs. foot. To look for refinement of somatomotor representations across early development, we mapped individual digit representations within the cortical hand representation (Table 2). To maximize the repetitions of digit stimulation and thereby our chance of finding digit representations, we stimulated only the right-hand digits during a full-scan session for newborn monkeys

M1 and M2. Digits were mapped in both hands for monkeys M3 and M4 in a full-scan session and only in the right hand for M7 at the end of the body-mapping scan session. In contrast to the adult-like hand representations (vs. face and foot) found in these newborn monkeys (Figs. 2 and 3 and *SI Appendix*, Figs. S1 and S2), responses to stimulation of individual digits were weak, and representations were not clearly differentiated spatially. In monkeys younger than 18 d, only small, focal regions representing a few contralateral digits were found within the hand representation of primary somatosensory (3a/b) cortex (Fig. 6A, left column). In monkey M1, representations of the contralateral thumb (red) and index finger (yellow), and a small representation of the middle finger (green) were found within the left hemisphere. In monkey M2, a representation of the middle finger and small representations of the thumb and pinkie were found within the left hemisphere. By a few months of age, contralateral representations of each finger could be clearly identified in both primary (3a/b) and secondary (SII) somatosensory cortex in left (Fig. 6A, middle column) and right (*SI Appendix*, Fig. S7) hemispheres and were in a similar location along the dorsal–ventral axis of the central sulcus as digit representations commonly found in adults (*SI Appendix*, Fig. S4A). Although evoked responses in these monkeys were relatively weak (<1% signal change) and similar in magnitude to newborns (Fig. 6B), the digit representations were more differentiated in 2- to 7-mo-old monkeys than in monkeys younger than 18 d [Fig. 6A, bottom row; mean Euclidean distance on group average maps = 1.29 (0.04) vs. 0.39 (0.02); paired t test, t (9) = −10.6449, $P < 0.0001$]. By 1 y 7 mo, these representations were more robust (Fig. 6A, right column) and the evoked responses were larger than in younger monkeys (Fig. 6B); however, the pinkie (D5) representation in M7 appears to be larger than would be expected based on the adult organization and extends dorsally into representations of the wrist and pad (*SI Appendix*, Fig. S4A). Because this monkey was reared normally and we did not see any extension into the wrist and pad region in any of the other 5 hemispheres, we assume M7's large pinkie representation may be due to partial stimulation of the wrist/pad during the pinkie blocks. Regardless, the digit representations were not any more differentiated between M7 and the 2- to 7-mo-old monkeys [(Fig. 6A, bottom row; mean Euclidean distance on group average maps = 1.28 (0.05)]; paired t test, t (9) = 0.22; $P = 0.83$]. Although our effective (spatial) sampling resolution was coarser for our infant monkeys due to their relatively smaller brains, we do not think this can account for the observed changes in digit representations. First, the cortical surface along the dorsal–ventral axis where digits are clearly differentiated in older monkeys spanned several millimeters in newborns, indicating that we still had a high enough spatial resolution to disambiguate signals from individual digits. Second, focal activity approximately the size of individual digit representations was observed from face stimulation in monkeys M1 and M3 (*SI Appendix*, Fig. S1), demonstrating that we were capable of detecting spatially focal activations at these ages. Third, we collected 3 times the data in infants compared with the 1-y 7-mo-old monkey. Together, these data suggest that the topographic map of hand digits may not be well differentiated at birth.

Lack of Cross-Modal Remapping in Sensory Deprivation. Despite the presence of an adult-like large-scale topographic organization of somatomotor cortex at birth, the early topographic organization is nevertheless more plastic than in adults, being capable of dramatic alteration following injury to peripheral input (39–42) or through dramatic changes in early somatomotor experience (43). However, the extent to which body representations are modifiable from alterations of other sensory modalities remains to be resolved. Studies in congenitally blind humans have shown somatosensory-evoked responses in visual cortex (44), suggesting that early deprivation in one sensory modality can lead to rewiring, such that other sensory modalities take over cortical
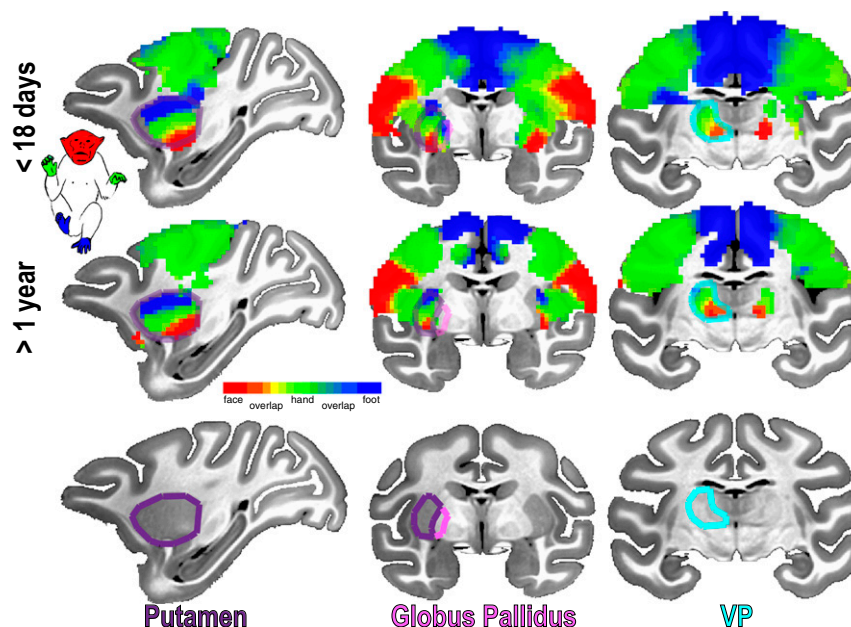
Fig. 5. Subcortical body map organization in newborns and juveniles. Representations of the contralateral body were found in the putamen, globus pallidus, and ventral posterior nucleus of the thalamus in newborns (M1 and M2), and these maps were comparable to the organization in juvenile monkeys (M7 and M8). Data threshold at a group average z statistic > 4 for the strongest IC in each vertex. See Fig. 1 for additional conventions.

territory typically performing computations related to the deprived modality. Here, we asked whether such cross-modal rewiring can be seen in monkeys and whether early experience (or lack thereof) is sufficient for driving such large-scale changes. As part of a separate experiment, we raised 2 monkeys (M5 and M6) for the first year of life (until 357 and 343 d, respectively) with visual experience restricted to diffuse light binocularly. Without form vision, behaviorally, touch became the dominant sensory modality in these animals. In contrast to control monkeys that rely on vision for navigation and identifying objects in their environment, these monkeys predominantly relied on touch both during and after the deprivation period. For example, when placed in an unfamiliar environment, normally reared monkeys will visually scan the layout. In contrast, these 2 monkeys surveyed the layout by making several passes around the perimeter, feeling the walls and floor with their hands. We asked whether there was a corresponding shift in the neural architecture dedicated to processing touch at postnatal days 426 and 438, respectively. In contrast to the stark behavioral shift, we found that body representations in these monkeys were comparable to age-matched control monkeys (Fig. 7). Representations of the face, hand, and foot were found throughout the central sulcus, frontal and parietal cortices, as well as subcortex. As seen in Fig. 7A, body part representations did not extend into either occipital or temporal cortex that typically responds to visual input. The extent of somatomotor maps also appeared comparable to age-matched control monkeys. Individual

digit representations were identified in visually deprived monkeys (Fig. 7B). The topographic organization of the hand digits was comparable to controls of similar ages. Digit representations were not significantly more (or less) differentiated in visually deprived monkeys than in 2- to 7-mo-old control monkeys [mean Euclidean distance on group average maps = 1.29 (0.05); paired t test, t (9) = 0.07; P = 0.94]. Together, these data suggest that an abnormal prioritization of touch starting at birth is insufficient to generate a large-scale somatomotor reorganization across sensory systems.

Discussion

Somatosensory and motor systems were found to be functionally organized to a remarkable degree in awake newborn macaques as young as 11 d postnatal. Here, we found spatially distinct activity in response to tactile stimulation of the contralateral face, hand, and foot within primary somatomotor cortex. This gradient covered somatotopic areas 3a/b and 1–2 as well as primary motor area M1/F1 and is consistent with the locations of face, hand, and foot representations shown from prior microelectrode recordings and intracortical microstimulation studies within the primary somatosensory (9–11) and motor cortex (4, 15, 16) of adult monkeys. Although we stimulated only 3 body parts, we expect that intervening body regions (e.g., torso and chest) are already represented. Indeed, in a subset of monkeys, we stimulated the lower back and found evoked activity between the hand and foot representation, consistent with the known organization in adults. Compared with

Table 2. Individual monkey scanning information for stimulation of hand digits

Monkey	Age, d	Stimulation paradigm	Body side stimulated	Hemisphere examined
M1	11	Manual stroke each digit	Right side only	Right side only
M2	17	Manual stroke each digit	Right side only	Right side only
M3	95	Manual stroke each digit	Both	Both
M4	202	Manual stroke each digit	Both	Both
M5	474	Manual stroke each digit	Both	Both
M6	486	Manual stroke each digit	Both	Both
M7	586	Manual stroke each digit	Right side only	Right side only
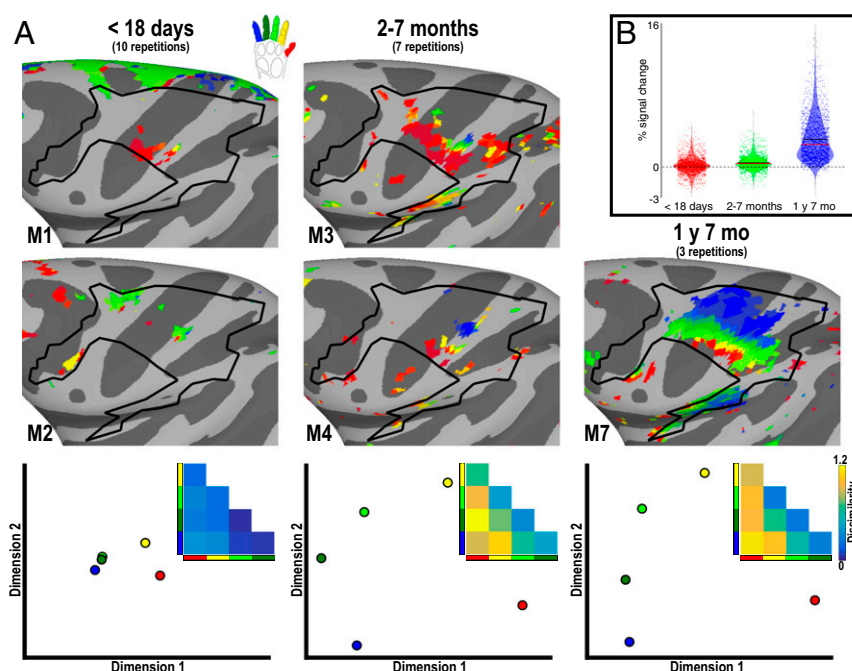
Fig. 6. Digit representations in newborns and juveniles. (*A*) With the exception of the thumb and index fingers, monkeys younger than 18 d old (M1 and M2) lacked spatially distinct representations of contralateral fingers in primary somatosensory cortex. In monkeys 2–7 mo of age (M3 and M4), representations of each digit were identified in primary (3a/b) and secondary (SII) somatosensory cortex. At 1 y 7 mo of age (M7), digit representations appeared more robust in primary and secondary somatosensory cortex and were also found within motor cortex. The black outline illustrates the extent of the group average hand IC map. MDS was computed across all voxels within the group average hand representation in the central sulcus. Data threshold of *P* < 0.0001, uncorrected, for the digit representation with the largest beta value. (*B*) Distribution of evoked responses from digit stimulation in the hand representation of primary somato-motor cortex for newborns, 2–7-mo-old, and 1-y 7-mo-old monkeys. Red line illustrates median, black line illustrates mean.

foot representations, the face and hand representations covered a greater extent of the cortical surface, consistent with their over-representation classically illustrated in homunculi. Our finding of somatomotor maps in neonates may appear at odds with a prior electrophysiological study that found neurons within primary somatosensory cortex of newborn monkeys to be unresponsive to tactile stimulation (7). However, these prior recordings were done under anesthesia, which may have dampened evoked responses. Interestingly, the magnitude of fMRI evoked responses to stimulation of the face, hand, and foot was weaker in our younger monkeys (up to 146 d) than in older monkeys (*SI Appendix*, Fig. S1), suggesting that while the large-scale body map organization is present, responses to tactile stimulation remain immature for the first several months. Our data are consistent with recent human studies that showed spatially distinct representations of the face, hand, and ankle within primary somatomotor cortex in 60-d-old (45) and preterm infants (46). Beyond primary somatomotor cortex, spatially distinct representations of the contralateral face, hand, and foot were observed throughout frontal, anterior parietal, and insular cortex as well as in subcortex in our newborn monkeys. The general anatomical location and organization of these body maps are in good agreement with prior findings from anatomical tracer and electrophysiological studies (2, 3, 6, 17, 21–26, 30, 33–38) as well as neuroimaging (12–14, 47). Despite the potential for considerable postnatal reorganization and refinement, the organization of these areas in newborns was indistinguishable from older juvenile monkeys, indicating that the large-scale somatomotor organization of the entire brain is already established at birth.

These maps likely form from a combination of molecular cues and activity-dependent sorting (48). Early in development, a combination of signaling molecules, transcriptional factors, and genes set up the axes and locations of cortical fields (49). Spontaneous and sensory-driven activity shape the size of cortical fields, map formation, and connectivity (50). Even in utero, there are extensive general motor movements both spontaneous (51, 52) and in response to environmental sensation (53) that could also play a role in the formation of these topographic maps (54). Still, at birth, motor movements are poorly controlled and imprecise, emphasizing a substantial role of postnatal experience in somatomotor development.

Despite an extensive large-scale body map organization, the finer-scale representations of individual hand digits were not well differentiated in newborn monkeys. In comparison, complete maps of hand digits were present in primary and secondary somatosensory cortex in 2- to 7-mo-old monkeys. This difference in the body map organization coincides with the maturation of fine motor skills. At birth, monkeys are behaviorally immature in motor function and lack adult-like precision and coordination. Motor movements become more precise and coordinated, especially for fingers, over first several months (55–57), paralleling the postnatal development of cortico-motoneuronal connections that innervate muscles (58–60). Thus, while the large-scale organization of the newborn brain was indistinguishable from older monkeys, our data are consistent with the possibility that refinement of somatomotor representations occurs over the course of the first year, paralleling the refinement of fine-motor movements. Still, responses in newborns were noisy, and there was notable variability in the extent of digit representations across older individuals. Future work is needed to resolve the degree to which refinement occurs over early development.

While early experience may refine the precision of somatomotor representations, the extent and large-scale organization of somatomotor systems were unaffected by dramatic shifts in early sensory experience. The somatomotor system is capable of massive reorganization from early somatosensory loss (39–42, 61). In humans with early vision loss, visual cortex can respond to other sensory modalities such as touch (43, 44, 62). We tested
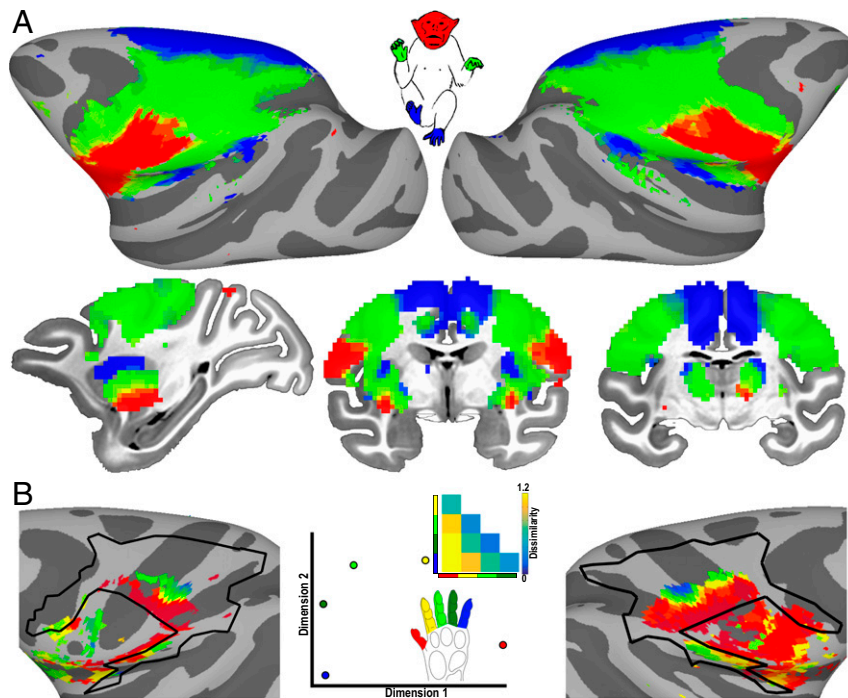
Fig. 7. No clear cross-modal reorganization in monkeys raised under visual form deprivation. (*A*) Body maps were found in 2 monkeys (M5 and M6) raised without visual form experience for the first year of life across (*Top*) cortex and (*Bottom*) subcortex. These monkeys primarily rely on touch for navigation and interacting with their environment. Despite this massive shift in sensory experience relative to control monkeys, the body map organization was indistinguishable from controls. (*B*) Digit representations were found in these monkeys comparable to juvenile control monkeys (Fig. 6 and *SI Appendix*, Fig. S7). Somatomotor activity was not observed in occipital cortex, suggesting that such drastic changes in early sensory experience were not sufficient to cause large-scale cross-modal rewiring. Body mapping threshold at *z* stat > 4.0 and digit mapping data threshold of *P* < 0.0001, uncorrected. See Fig. 1 for additional conventions.

whether such cross-modal plasticity occurred in monkeys raised for the first year with visual experience restricted to diffuse light. In contrast to control monkeys that primarily relied on vision for navigation and interacting with their environment, these monkeys relied on touch even after the deprivation period. Despite the reliance on touch over other sensor modalities for behavior, the large-scale organization of the somatomotor system in these monkeys was indistinguishable from that in control monkeys, demonstrating that early sensory deprivation alone was insufficient to induce large-scale cross-modal reorganization. In contrast to prior findings in early-blind humans (43, 44, 62), in whom tactile stimulation evoked activity within occipital cortex, no increased activity in occipital or temporal cortex was observed in these monkeys from face, foot, or hand stimulation. The large shift in these monkeys' sensory experience was not driven by trauma to the eye or peripheral pathways that typically induce sensory loss in human studies, suggesting that spontaneous activity within intact anatomical pathways (or simply the experience of diffuse light) may limit the degree of cross-modal plasticity.

A protoarchitecture of body maps may support subsequent experience-driven refinement throughout the somatomotor system. In addition to representations of individual body parts, mature motor cortex contains functional domains specialized for the execution of coordinated movements across multiple joints. These domains emphasize different complex, ethologically relevant, categories of action (63) and are localized to stereotypical locations of body maps across individuals. Such functional specialization can emerge in self-organizing simulated networks trained on a set of complex movements, without requiring domain-specific priors (64). We speculate that the early topographic organization of the somatomotor system observed in newborn monkeys provides the scaffolding for the subsequent development of these ethological

functional domains, and also permits the myriad of potential complex, coordinated behaviors that develop based on an individual's particular experience and needs (65).

This extensive body map organization parallels our recent findings that the entire visual system is retinotopically organized at birth (66) and likely supports experience-driven development of behaviorally relevant domains, such as those that selectively respond to text or faces (67, 68). Together, these findings illustrate that topographic maps of sensory space are a fundamental and pervasive (Fig. 8) organizing principle of the brain, and they play an important role in development by guiding and constraining experience-driven refinement and specialization.

Materials and Methods

fMRI studies were carried out on 11 *Macaca mulatta* monkeys, 5 females and 6 males, between the ages of 11 and 981 d. All procedures were approved by the Harvard Medical School Animal Care and Use Committee and conformed to NIH guidelines for the humane care and use of laboratory animals (69). All monkeys were born in our laboratory. One monkey (M9) was cohoused with their mother in a room with other monkeys for the first 4 mo, and then cohoused with other juveniles, also in a room with other monkeys. As part of separate experiments, all other monkeys were hand reared by humans for the first year, and then were cohoused with other juveniles. Two of the hand-reared monkeys (M5 and M6) were raised under conditions of visual form deprivation via eyelid suturing for the first year. Experiments were conducted in these 2 monkeys after eyelid reopening. For scanning, all monkeys were alert, and they were scanned in a primate chair that allowed them to move their bodies and limbs freely, but their heads were restrained in a forward-looking position by a padded helmet with a chin strap that delivered juice. To keep monkeys complacent, they were rewarded with juice (1 bolus/2 s) continuously throughout each scan.

Tactile Stimulation. For monkeys M1 to M8, tactile stimulation was performed using air puffs for face stimulation and gentle manual stroking for other body
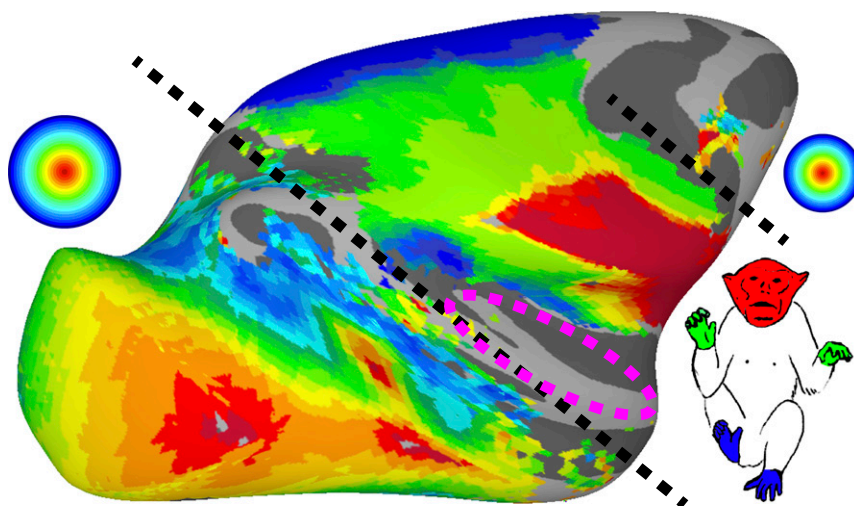
Fig. 8. Importance of being topographic. Topographic representations of sensory spaces cover most of the cortical surface. As illustrated by a group average (*n* = 6) eccentricity map (32), the posterior half of the brain and an anterior part of the arcuate sulcus (FEF) comprise retinotopic representations of visual space. As illustrated by a group average (*n* = 8) body map, anterior parietal, frontal, and insular cortex comprise topographic representations of the body. These retinotopic (62) and somatomotor (current study) maps are present at birth. The black dashed lines differentiate retinotopic and somatomotor body maps. As illustrated by the magenta dashed circle, several tonotopic maps span the lower bank of the lateral sulcus (81).

part stimulation (Table 1). The tubes delivering air puffs were focused on each cheek between the upper lip and nose. For foot (and hand) stimulation, the experimenter stroked the entire extent of the glabrous foot including toes (palm of hand including fingers). For monkey M9, hand and foot responses were measured via air puffs. This method was found to be non-optimal because the tubes that delivered air puffs kinked during the scan due to monkey movement, resulting in unreliable stimulation. Body maps are shown for monkey M9, but because of this different method of body part stimulation and unreliable stimulation of the feet and hands, data were not included in the direct comparisons between newborns and juvenile for Figs. 3*A*, 4, and 5. For the 2 youngest monkeys (M1 and M2), hand, foot, and face responses were measured for the right side of the body only, to increase the number of repetitions collected. For monkeys M3 to M8, hand, foot, lower back (just above the tail), and face responses were measured bilaterally. Each scan comprised blocks of unilateral stimulation of individual body parts; block length was 20 s, with 20 s of no-stimulation interleaved. Seven monkeys (M1 to M7) participated in a finger mapping experiment where responses to manual stroking of the glabrous thumb, index, middle, ring, and pinkie fingers were measured (Table 2). For the 2 youngest monkeys (M1 and M2) and M7, responses were measured to stimulation of digits only in the right hand, again to increase the number of repetitions collected. For the other 5 monkeys (M3 to M6), responses to stimulation of digits in both hands were mapped. Monkeys were rewarded with juice every couple of seconds continuously throughout the scan.

In a separate control experiment, juice was delivered in 20-s blocked epochs interleaved with 20 s of no tactile stimulation to 3 monkeys (M1, M10, and M11). Fifteen repetitions of juice stimulation were collected in each monkey. The goal of this experiment was to identify activity from a regression analysis specifically related to the administration of juice and stimulation of the mouth, tongue, and teeth. Because juice was delivered continuously every couple of seconds in the main tactile mapping experiment, juice-related activity could not be modeled in the regression analysis.

Scanning. Monkeys were scanned in a 3-T TimTrio scanner with an AC88 gradient insert using 4-channel surface coils (custom-made by Azma Mareyam at the Martinos Imaging Center). Each tactile stimulation scan session consisted of 10 to 12 functional scans. We used a repetition time of 2 s, echo time of 13 ms, flip angle of 72°, integrated parallel acquisition technique (iPAT) = 2, 1-mm isotropic voxels, matrix size of 96 × 96 mm, and 67 contiguous sagittal slices. To enhance contrast (70, 71), we injected 12 mg/kg MIONs (Feraheme; AMAG Pharmaceuticals) in the saphenous vein just before scanning.

General Preprocessing. Functional scan data were analyzed using Analysis of Functional NeuroImages (AFNI; RRID:nif-0000-00259) (72), SUMA (73), Free-surfer (Freesurfer; RRID:nif-0000-00304) (74, 75), JIP Analysis Toolkit (written by Joseph Mandeville, Harvard Medical School, Boston, MA), and MATLAB

(Mathworks; RRID:nlx_153890). Each scan session for each monkey was analyzed separately. All images from each scan session were motion corrected and aligned to a single timepoint for that session using AFNI. Data were detrended and spatially filtered using a Gaussian filter of 2-mm full width at half-maximum to increase the signal-to-noise ratio while preserving spatial specificity. All images were masked to exclude voxels that fell outside of the brain. Each scan was normalized to its mean. Data were registered using a 2-step linear then nonlinear alignment approach (JIP analysis toolkit) to a standard anatomical template (NMT; ref. 76) for all monkeys. First, a 12-parameter linear registration was performed between the mean echo-planar imaging (EPI) image for a given session and a high-resolution anatomical image. Next, a nonlinear, diffeomorphic registration was conducted. To improve registration accuracy of ventral cortex, masks were manually drawn that excluded the cerebellum for both EPIs and anatomical images prior to registration.

Regression Analysis. A multiple regression analysis [AFNI's 3dDeconvolve (72)] in the framework of a general linear model (GLM) (77) was performed on the tactile stimulation mapping experiments for each monkey separately. Each stimulus condition was modeled with a MION-based hemodynamic response function (70). Additional regressors that accounted for variance due to baseline shifts between time series, linear drifts, and head motion parameter estimates were also included in the regression model. Due to the time course normalization, beta coefficients were scaled to reflect percent signal change. Since MION inverts the signal, the sign of beta values was inverted to follow normal fMRI conventions of increased activity represented by positive values. Maps of beta coefficients for each body part stimulated set to a threshold of *P* < 0.0001 (uncorrected).

ICA. A 2D (space × time) ICA (FSL's MELODIC using default settings) was performed on the concatenated preprocessed and brain-masked runs for each scan session. ICA is a special case of blind source separation where signals throughout the brain are parsed into statistically independent components. This analysis decomposes each space × time matrix into pairs of temporal and spatial subcomponents. This analysis assumes that the subcomponents are non-Gaussian signals and are statistically independent from each other. The analysis was restricted to voxels that fell within a whole-brain mask. Between 15 and 40 components were identified in each scan session. Spatial IC maps were then reconstructed from each component to visualize the regions of the brain whose signals most contributed to each component. For each scan session (i.e., monkey), spatial IC maps were identified based on correspondence with face, hand, and foot activations from the group average activity (beta) maps as well as similarity to prior reports on the topographic organization of primary somatomotor cortex in adults (*SI Appendix*, Fig. S4 and ref. 3). These spatial maps were transformed to *z* statistics by dividing the raw IC estimate by the voxelwise noise SD and

were threshold at $z > 4.00$. Because the transformation to voxelwise Z scores can result in an uncontrolled false-positive rate under the null-hypothesis (78), we verified that the median posterior probability (P) of voxelwise activation (vs. null) for each z-threshold IC map > 0.95.

Body Map Analysis. Topographic maps of the body were derived from the face, hand, and foot spatial IC maps. For each voxel, the z statistics of the face, hand, and foot ICs were extracted and were normalized to the maximal response. These normalized responses were linearly interpolated into a 100-point 3-dimensional scale with each dimension ranging between 0 and 1. The first, second, and third dimensions corresponded to the weighting of face, hand, and foot ICs, respectively; e.g., "1 0 0" corresponded to a weighting of 100% face IC and 0% foot and hand, and "0 1 0" corresponded to a weighting of 100% hand IC and 0% face and foot. These 3-dimensional values were visualized on an RGB color scale such that "1 0 0" corresponded to red, "0 1 0" corresponded to green, and "0 0 1" corresponded to blue.

Multivoxel Similarity Analyses. The spatial similarity of face, hand, and foot representations was compared by (Pearson) correlating the IC maps across monkeys then averaging across hemispheres. This yielded a symmetric 27×27 (9 monkeys $\times$ 3 body part) similarity matrix (Fig. 3C). Classical MDS was applied on the Euclidean distances between these correlations and the first 2 principal dimensions were visualized. The spatial similarity of digit representations was compared by correlating the beta maps of thumb, pointed, middle, index, and pinkie fingers within the group average IC map across monkeys. Because there was a clear difference in the digit maps between newborns and juveniles, data were grouped into 3 age ranges (<18 d, 2–7 mo, and >1 y), and MDS was applied on each group separately. For each group, the first 2 components were visualized (Figs. 6 and 7 and *SI Appendix*, Fig. S7). The distances between digit representations were compared between groups with nonpaired, 2-tailed t tests.

Comparison to Atlas. To directly compare visual field maps across monkeys, each monkey's data were aligned to a standard template (NMT) surface using nonlinear registration (JIP Analysis Toolkit). Group average maps were compared with the borders of a digitized version (79) of the Saleem and Logothetis (80) macaque atlas that was aligned to the NMT anatomy (https://github.com/jms290/NMT; ref. 76).

Quantification and Statistical Analyses. In Figs. 1, 6, and 7 and *SI Appendix*, Figs. S1, S3, S5, and S7, spatial maps of beta coefficients were set to a threshold of $P < 0.0001$ (uncorrected). In Figs. 1–3, 5, 7, and 8 and *SI Appendix*, Figs. S2–S6, IC and gradient maps were set to a threshold of z statistics > 4.00. These z statistics were computed by dividing the raw IC estimate by the voxelwise noise SD. For data presented in Fig. 3C, Pearson correlations were computed on the spatial pattern of z statistics across the entire brain between monkeys. A dissimilarity matrix (1-r) was created from these correlations between all 9 monkeys in the main experiment. Classical MDS was applied on the Euclidean distances between these correlations and the first 2 principal dimensions were visualized. For data presented in Figs. 6 and 7 and *SI Appendix*, Fig. S7, a similar analysis was performed on the beta weights for individual digits within the hand representation of primary somato-motor cortex.

Data and Code Availability. Data will be made available upon request. We used publicly available image analysis software as listed in Tables 1 and 2 and standard MATLAB functions for analysis.

1. J. H. Kaas, Topographic maps are fundamental to sensory processing. *Brain Res. Bull.* **44**, 107–112 (1997).
2. V. Raos, G. Franchi, V. Gallese, L. Fogassi, Somatotopic organization of the lateral part of area F2 (dorsal premotor cortex) of the macaque monkey. *J. Neurophysiol.* **89**, 1503–1518 (2003).
3. A. M. Seelke et al., Topographic maps within Brodmann's area 5 of macaque monkeys. *Cereb. Cortex* **22**, 1834–1850 (2012).
4. P. L. Strick, J. B. Preston, Multiple representation in the primate motor cortex. *Brain Res.* **154**, 366–370 (1978).
5. Y. C. Wong, H. C. Kwan, W. A. MacKay, J. T. Murphy, Spatial organization of precentral cortex in awake primates. I. Somatosensory inputs. *J. Neurophysiol.* **41**, 1107–1119 (1978).
6. J. L. Vitek, J. Ashe, M. R. DeLong, G. E. Alexander, Physiologic properties and somatotopic organization of the primate motor thalamus. *J. Neurophysiol.* **71**, 1498–1513 (1994).
7. L. A. Krubitzer, J. H. Kaas, Responsiveness and somatotopic organization of anterior parietal field 3b and adjoining cortex in newborn and infant monkeys. *Somatosens. Mot. Res.* **6**, 179–205 (1988).
8. T. P. Pons, J. H. Kaas, Corticocortical connections of area 2 of somatosensory cortex in macaque monkeys: A correlative anatomical and electrophysiological study. *J. Comp. Neurol.* **248**, 313–335 (1986).
9. M. M. Merzenich, J. H. Kaas, M. Sur, C. S. Lin, Double representation of the body surface within cytoarchitectonic areas 3b and 1 in "SI" in the owl monkey (*Aotus trivirgatus*). *J. Comp. Neurol.* **181**, 41–73 (1978).
10. J. H. Kaas, R. J. Nelson, M. Sur, C. S. Lin, M. M. Merzenich, Multiple representations of the body within the primary somatosensory cortex of primates. *Science* **204**, 521–523 (1979).
11. R. J. Nelson, M. Sur, D. J. Felleman, J. H. Kaas, Representations of the body surface in postcentral parietal cortex of *Macaca fascicularis*. *J. Comp. Neurol.* **192**, 611–643 (1980).
12. T. Hayashi, S. Konishi, I. Hasegawa, Y. Miyashita, Short communication: Mapping of somatosensory cortices with functional magnetic resonance imaging in anaesthetized macaque monkeys. *Eur. J. Neurosci.* **11**, 4451–4456 (1999).
13. S. Sharma, P. A. Fiave, K. Nelissen, Functional MRI responses to passive, active, and observed touch in somatosensory and insular cortices of the macaque monkey. *J. Neurosci.* **38**, 3689–3707 (2018).
14. E. Disbrow, T. P. Roberts, D. Slutsky, L. Krubitzer, The use of fMRI for determining the topographic organization of cortical fields in human and nonhuman primates. *Brain Res.* **829**, 167–173 (1999).
15. H. C. Kwan, W. A. Mackay, J. T. Murphy, Y. C. Wong, An intracortical microstimulation study of output organization in precentral cortex of awake primates. *J. Physiol. (Paris)* **74**, 231–233 (1978).
16. H. C. Kwan, W. A. MacKay, J. T. Murphy, Y. C. Wong, Spatial organization of precentral cortex in awake primates. II. Motor outputs. *J. Neurophysiol.* **41**, 1120–1131 (1978).
17. L. Krubitzer, J. Clarey, R. Tweedale, G. Elston, M. Calford, A redefinition of somatosensory areas in the lateral sulcus of macaque monkeys. *J. Neurosci.* **15**, 3821–3839 (1995).
18. P. R. Manger, T. M. Woods, E. G. Jones, Representation of face and intra-oral structures in area 3b of macaque monkey somatosensory cortex. *J. Comp. Neurol.* **371**, 513–521 (1996).
19. H. P. Killackey, H. J. Gould, 3rd, C. G. Cusick, T. P. Pons, J. H. Kaas, The relation of corpus callosum connections to architectonic fields and body surface maps in sensorimotor cortex of New and Old World monkeys. *J. Comp. Neurol.* **219**, 384–419 (1983).
20. N. Jain, H. X. Qi, K. C. Catania, J. H. Kaas, Anatomic correlates of the face and oral cavity representations in the somatosensory cortical area 3b of monkeys. *J. Comp. Neurol.* **429**, 455–468 (2001).
21. H. Sakata, Y. Takaoka, A. Kawarasaki, H. Shibutani, Somatosensory properties of neurons in the superior parietal cortex (area 5) of the rhesus monkey. *Brain Res.* **64**, 85–102 (1973).
22. V. B. Mountcastle, J. C. Lynch, A. Georgopoulos, H. Sakata, C. Acuna, Posterior parietal association cortex of the monkey: Command functions for operations within extrapersonal space. *J. Neurophysiol.* **38**, 871–908 (1975).
23. T. P. Pons, P. E. Garraghty, C. G. Cusick, J. H. Kaas, A sequential representation of the occiput, arm, forearm and hand across the rostrocaudal dimension of areas 1, 2 and 5 in macaque monkeys. *Brain Res.* **335**, 350–353 (1985).
24. M. Gentilucci et al., Somatotopic representation in inferior area 6 of the macaque monkey. *Brain Behav. Evol.* **33**, 118–121 (1989).
25. G. Rizzolatti, C. Scandolara, M. Gentilucci, R. Camarda, Response properties and behavioral modulation of "mouth" neurons of the postarcuate cortex (area 6) in macaque monkeys. *Brain Res.* **225**, 421–424 (1981).
26. K. Kurata, J. Tanji, Premotor cortex neurons in macaques: Activity before distal and proximal forelimb movements. *J. Neurosci.* **6**, 403–411 (1986).
27. S. P. Wise, D. Boussaoud, P. B. Johnson, R. Caminiti, Premotor and parietal cortex: Corticocortical connectivity and combinatorial computations. *Annu. Rev. Neurosci.* **20**, 25–42 (1997).
28. M. C. Park, A. Belhaj-Saïf, M. Gordon, P. D. Cheney, Consistent features in the forelimb representation of primary motor cortex in rhesus macaques. *J. Neurosci.* **21**, 2784–2792 (2001).
29. M. H. Schieber, Motor cortex and the distributed anatomy of finger movements. *Adv. Exp. Med. Biol.* **508**, 411–416 (2002).
30. C. G. Cusick, H. J. Gould, 3rd, Connections between area 3b of the somatosensory cortex and subdivisions of the ventroposterior nuclear complex and the anterior pulvinar nucleus in squirrel monkeys. *J. Comp. Neurol.* **292**, 83–102 (1990).
31. T. P. Pons, J. H. Kaas, Connections of area 2 of somatosensory cortex with the anterior pulvinar and subdivisions of the ventroposterior complex in macaque monkeys. *J. Comp. Neurol.* **240**, 16–36 (1985).
32. M. J. Arcaro, M. S. Livingstone; Retinotopic Organization of Scene Areas in Macaque Inferior Temporal Cortex, Retinotopic organization of scene areas in macaque inferior temporal cortex. *J. Neurosci.* **37**, 7373–7389 (2017).

Arcaro et al.

33. H. Künzle, Bilateral projections from precentral motor cortex to the putamen and other parts of the basal ganglia. An autoradiographic study in *Macaca fascicularis*. *Brain Res.* **88**, 195–209 (1975).

34. A. W. Flaherty, A. M. Graybiel, Output architecture of the primate putamen. *J. Neurosci.* **13**, 3222–3237 (1993).

35. A. Nambu, K. Kaneda, H. Tokuno, M. Takada, Organization of corticostriatal motor inputs in monkey putamen. *J. Neurophysiol.* **88**, 1830–1842 (2002).

36. S. Yoshida, A. Nambu, K. Jinnai, The distribution of the globus pallidus neurons with input from various cortical areas in the monkeys. *Brain Res.* **611**, 170–174 (1993).

37. C. Asanuma, W. R. Thach, E. G. Jones, Anatomical evidence for segregated focal groupings of efferent cells and their terminal ramifications in the cerebellothalamic pathway of the monkey. *Brain Res.* **286**, 267–297 (1983).

38. J. H. Kaas, R. J. Nelson, M. Sur, R. W. Dykes, M. M. Merzenich, The somatotopic organization of the ventroposterior thalamus of the squirrel monkey, *Saimiri sciureus*. *J. Comp. Neurol.* **226**, 111–140 (1984).

39. M. Devor, P. D. Wall, Reorganisation of spinal cord sensory map after peripheral nerve injury. *Nature* **276**, 75–76 (1978).

40. M. M. Merzenich *et al.*, Topographic reorganization of somatosensory cortical areas 3b and 1 in adult monkeys following restricted deafferentation. *Neuroscience* **8**, 33–55 (1983).

41. P. E. Garraghty, J. H. Kaas, Large-scale functional reorganization in adult monkey cortex after peripheral nerve injury. *Proc. Natl. Acad. Sci. U.S.A.* **88**, 6976–6980 (1991).

42. T. P. Pons *et al.*, Massive cortical reorganization after sensory deafferentation in adult macaques. *Science* **252**, 1857–1860 (1991).

43. M. C. Stoeckel, R. J. Seitz, C. M. Buetefisch, Congenitally altered motor experience alters somatotopic organization of human primary motor cortex. *Proc. Natl. Acad. Sci. U.S.A.* **106**, 2395–2400 (2009).

44. N. Sadato *et al.*, Activation of the primary visual cortex by Braille reading in blind subjects. *Nature* **380**, 526–528 (1996).

45. A. N. Meltzoff, J. N. Saby, P. J. Marshall, Neural representations of the body in 60-day-old human infants. *Dev. Sci.* **22**, e12698 (2019).

46. S. Dall'Orso *et al.*, Somatotopic mapping of the developing sensorimotor cortex in the preterm human brain. *Cereb. Cortex* **28**, 2507–2515 (2018).

47. K. Nelissen, W. Vanduffel, Grasping-related functional magnetic resonance imaging brain responses in the macaque monkey. *J. Neurosci.* **31**, 8220–8229 (2011).

48. T. McLaughlin, D. D. O'Leary, Molecular gradients and development of retinotopic maps. *Annu. Rev. Neurosci.* **28**, 327–355 (2005).

49. D. D. O'Leary, S. J. Chou, S. Sahara, Area patterning of the mammalian cortex. *Neuron* **56**, 252–269 (2007).

50. L. E. White, D. Fitzpatrick, Vision and cortical map development. *Neuron* **56**, 327–338 (2007).

51. J. I. de Vries, G. H. Visser, H. F. Prechtl, The emergence of fetal behaviour. II. Quantitative aspects. *Early Hum. Dev.* **12**, 99–120 (1985).

52. A. Kurjak *et al.*, The assessment of fetal neurobehavior by three-dimensional and four-dimensional ultrasound. *J. Matern. Fetal Neonatal Med.* **21**, 675–684 (2008).

53. V. Marx, E. Nagy, Fetal behavioural responses to maternal voice and touch. *PLoS One* **10**, e0129118 (2015).

54. J. Fagard, R. Esseily, L. Jacquey, K. O'Regan, E. Somogyi, Fetal origin of sensorimotor behavior. *Front. Neurorobot.* **12**, 23 (2018).

55. R. Castell, G. Sackett, Motor behaviors of neonatal rhesus monkeys: Measurement techniques and early development. *Dev. Psychobiol.* **6**, 191–202 (1973).

56. J. H. Robinette, J. Ha, C. Kimpo, G. Sackett, Climbing test to measure gross motor development in monkeys. *Am. J. Primatol.* **35**, 319–326 (1995).

57. D. G. Lawrence, D. A. Hopkins, The development of motor control in the rhesus monkey: Evidence concerning the role of corticomotoneuronal connections. *Brain* **99**, 235–254 (1976).

58. H. G. J. M. Kuypers, "Anatomy of the descending pathways" in *Handbook of Physiology, Section 1: The Nervous System, Volume II: Motor Control*, V. B. Brooks, Ed. (American Physiological Society, Bethesda), pp 597–666 (1981).

59. J. Armand, E. Olivier, S. A. Edgley, R. N. Lemon, Postnatal development of corticospinal projections from motor cortex to the cervical enlargement in the macaque monkey. *J Neurosci.* **17**, 251–266 (1997).

60. J. Rathelot, P. L. Strick, Subdivisions of primary motor cortex based on cortico-motoneuronal cells. *Proc. Natl. Acad. Sci. U.S.A.* **106**, 918–923 (2009).

61. N. Jain, H. X. Qi, C. E. Collins, J. H. Kaas, Large-scale reorganization in the somatosensory cortex and thalamus after sensory loss in macaque monkeys. *J. Neurosci.* **28**, 11042–11060 (2008).

62. N. Sadato, M. Hallett, fMRI occipital activation by tactile stimulation in a blind man. *Neurology* **52**, 423 (1999).

63. M. S. A. Graziano, Ethological action maps: A paradigm shift for the motor cortex. *Trends Cogn. Sci.* **20**, 121–132 (2016).

64. T. N. Aflalo, M. S. Graziano, Possible origins of the complex topographic organization of motor cortex: Reduction of a multidimensional space onto a two-dimensional array. *J. Neurosci.* **26**, 6288–6297 (2006).

65. M. K. L. Baldwin, D. F. Cooke, A. B. Goldring, L. Krubitzer, Representations of fine digit movements in posterior and anterior parietal cortex revealed using long-train intracortical microstimulation in macaque monkeys. *Cereb. Cortex* **28**, 4244–4263 (2018).

66. M. J. Arcaro, M. S. Livingstone, A hierarchical, retinotopic proto-organization of the primate visual system at birth. *eLife* **6**, e26196 (2017).

67. M. J. Arcaro, P. F. Schade, J. L. Vincent, C. R. Ponce, M. S. Livingstone, Seeing faces is necessary for face-domain formation. *Nat. Neurosci.* **20**, 1404–1412 (2017).

68. K. Srihasam, J. L. Vincent, M. S. Livingstone, Novel domain formation reveals proto-architecture in inferotemporal cortex. *Nat. Neurosci.* **17**, 1776–1783 (2014).

69. National Research Council, *Guide for the Care and Use of Laboratory Animals* (National Academies Press, Washington, DC, ed. 8, 2011).

70. F. P. Leite *et al.*, Repeated fMRI using iron oxide contrast agent in awake, behaving macaques at 3 tesla. *Neuroimage* **16**, 283–294 (2002).

71. W. Vanduffel *et al.*, Visual motion processing investigated using contrast agent-enhanced fMRI in awake behaving monkeys. *Neuron* **32**, 565–577 (2001).

72. R. W. Cox, AFNI: Software for analysis and visualization of functional magnetic resonance neuroimages. *Comput. Biomed. Res.* **29**, 162–173 (1996).

73. Z. S. Saad, R. C. Reynolds, Suma. *Neuroimage* **62**, 768–773 (2012).

74. A. M. Dale, B. Fischl, M. I. Sereno, Cortical surface-based analysis. I. Segmentation and surface reconstruction. *Neuroimage* **9**, 179–194 (1999).

75. B. Fischl, M. I. Sereno, A. M. Dale, Cortical surface-based analysis. II: Inflation, flattening, and a surface-based coordinate system. *Neuroimage* **9**, 195–207 (1999).

76. J. Seidlitz *et al.*, A population MRI brain template and analysis tools for the macaque. *Neuroimage* **170**, 121–131 (2018).

77. K. J. Friston, C. D. Frith, R. Turner, R. S. Frackowiak, Characterizing evoked hemodynamics with fMRI. *Neuroimage* **2**, 157–165 (1995).

78. C. F. Beckmann, S. M. Smith, Probabilistic independent component analysis for functional magnetic resonance imaging. *IEEE Trans. Med. Imaging* **23**, 137–152 (2004).

79. C. Reveley *et al.*, Three-dimensional digital template atlas of the macaque brain. *Cereb. Cortex* **27**, 4463–4477 (2017).

80. K. S. Saleem, N. K. Logothetis, *A Combined MRI and Histology Atlas of the Rhesus Monkey Brain in Stereotaxic Coordinates* (Horizontal, Coronal and Sagittal Series, Elsevier Academic Press, San Diego, ed. 2, 2012).

81. C. I. Petkov, C. Kayser, M. Augath, N. K. Logothetis, Functional imaging reveals numerous fields in the monkey auditory cortex. *PLoS Biol.* **4**, e215 (2006).

NEUROSCIENCE